

Heuristic Learning for Co-Design Scheme of Optimal Sequential Attack

Xiaoyu Luo[†], Haoxuan Pan[†], Chongrong Fang[†], Chengcheng Zhao[‡], Peng Cheng[‡], and Jianping He[†]

Abstract—This paper considers a novel co-design problem of the optimal *sequential* attack, whose attack strategy changes with the time series, and in which the *sequential* attack selection strategy and *sequential* attack signal are simultaneously designed. Different from the existing attack design works that separately focus on attack subsets or attack signals, the joint design of the attack strategy poses a huge challenge due to the deep coupling relation between the *sequential* attack selection strategy and *sequential* attack signal. In this manuscript, we decompose the sequential co-design problem into two equivalent sub-problems. Specifically, we first derive an analytical closed-form expression between the optimal attack signal and the sequential attack selection strategy. Furthermore, we prove the finite-time inverse convergence of the critical parameters in the injected optimal attack signal by discrete-time Lyapunov analysis, which enables the efficient off-line design of the attack signal and saves computing resources. Finally, we exploit its relationship to design a heuristic two-stage learning-based joint attack algorithm (HTL-JA), which can accelerate realization of the attack target compared to the one-stage proximal-policy-optimization-based (PPO) algorithm. Extensive simulations are conducted to show the effectiveness of the injected optimal sequential attack.

Index Terms—False data injection attacks, learning-based methods, attack selection strategy, convergence

I. INTRODUCTION

SECURITY issues are becoming increasingly prominent in networked control systems (NCSs) as network technologies are extensively used to connect physical components within a control loop [1]. In NCSs, false data injection (FDI) — whereby an adversary injects false data by manipulating sensor readings or communication channels — is a commonly encountered form of cyber attack [2]. Crucially, through an FDI attack, an adversary can cause significant damage to control components while remaining undetected. For instance, on June 27, 2022, anonymous hacker organization Gonjeshke Darande carried out cyber attacks against Iran’s steel industry such that a heavy machine on a billet production line broke down and caused a fire [3]. As a result, the steel industry had to halt production, leading to lots of economic losses.

[†]: The Department of Automation, Shanghai Jiao Tong University, and Key Laboratory of System Control and Information Processing, Ministry of Education of China, Shanghai 200240, China. E-mail: xyl.sjtu@sjtu.edu.cn, panhaoxuan@sjtu.edu.cn, crfang@sjtu.edu.cn, jphe@sjtu.edu.cn.

[‡]: The State Key Laboratory of Industrial Control Technology and Institute of Cyberspace Research, Zhejiang University, China. E-mail: chengchengzhao@zju.edu.cn, lunarheart@zju.edu.cn.

A. Motivations

Considerable efforts have been devoted to studying the effects of potential FDI attacks [4]–[8] and designing the optimal FDI attack strategies [9]–[11]. For instance, Chen *et al.* [9] found an optimal attack strategy to balance the control objective and the detection avoidance objective. Li *et al.* derived the optimal linear attack vector injected in the sensor readings to degrade the system estimation performance [10]. Jafari *et al.* [11] studied an optimal false data injection attack (OFDIA) on automatic generation control (AGC) in power systems to destroy the frequency stability. Most of these works focus on the design of the injected optimal attack signal to meet the given objective function. Besides, there are some researchers aiming at developing the FDI attack selection strategy [12]–[15]. Wu *et al.* solved an optimal switching data injection attack design problem where only one actuator is compromised each time to minimize the quadratic cost function [12]. In [15], the adversary with limited capability aims to select a subset of agents and manipulate their local multi-dimensional states to maximize the consensus convergence error by utilizing the submodularity optimization theory. It shows distinct attack effects under different attack selection strategies.

Note that there exist three interesting problems worthy of further investigation. The first one is to explore the relationship between the injected attack signal and the attack selection strategy. For an adversary, selecting which agent to compromise and how much attack signal to inject are two key tasks. Usually, they are coupled and integrated into the system. It is significant to build an analytic expression for both and analyze how the attack selection strategy influences the injected attack signal. With this relationship, it is beneficial to probe the adversary’s potential capability and predict its possible behavior. It is worth noting that few works focus on excavating the analytic relationship between them. The second one is to excavate the convergence property of the injected optimal attack signal. It is intriguing and promising to demonstrate the characteristic of the injected attack signal. Once its convergence property is excavated, the adversary can effectively inject attack signal and save unnecessary computing resources to maximize the malicious effects. The third one is to tackle the sequential attack selection problem as time varies instead of a fixed compromised subset. It is more practical for an intelligent adversary to maximize the attack effects with time-varying attack selection strategies. For example, in smart grids, many substations can be

compromised sequentially, whose combinations are prone to cause severe large-scale blackouts [7]. Additionally, from the perspective of the system protection, it is advantageous to analyze the potential system's vulnerability and design resilient algorithms to improve the system's security.

B. Contributions

In this paper, we study the co-design problem of optimal sequential FDI attack where the adversary aims to specify how to select the compromised agent and inject the attack signal sequentially. Concretely, we derive the relationship between the injected optimal sequential attack signal and the attack selection strategy. Meanwhile, we desire to seek the potential convergence property of the injected attack signal where the adversary aims to steer the system state value to an expected malicious one in a discrete-time system. Compared to our conference version [16], we extend the sequential attack signal design problem to the sequential attack selection problem and propose a heuristic two-stage learning-based joint attack algorithm (HTL-JA) to reach optimal performance. Moreover, we significantly enrich the related works, motivation and simulation results. The main contributions are summarized as follows.

- We construct a sequential joint attack design framework where the adversary selects the sequential attack subsets and injects sequential attack signal over sampling times to drive the system state to a desired malicious one.
- We derive an analytical closed-form expression between the optimal sequential attack signal and the attack selection strategy, in which they are deeply coupled. Moreover, we theoretically characterize the finite-time inverse convergence of the critical parameters in the obtained optimal sequential attack signal via the discrete-time Lyapunov analysis.
- We propose a heuristic two-stage learning-based joint attack algorithm (HTL-JA), which contributes to acquiring the sequential attack subset and speeding up the realization of the attack target.

C. Paper Organization

The rest of the paper is organized as follows. Related works are reviewed in Section II. Section III introduces the system model and the adversary model, and formulates the FDI attack co-design problem. In Section IV, the optimal sequential attack signal is designed. Section V proposes a heuristic two-stage learning-based attack selection strategy. Simulation results are presented in Section VI. Finally, we conclude our work in Section VII.

Notations. Let \mathbb{R} denote the set of real numbers. For a vector $l_1 \in \mathbb{R}^p$, we have $\|l_1\|_R^2 \triangleq l_1^T R l_1$ with the positive definite weight matrix R . We denote I_n and 1_n as the n -dimensional diagonal unit matrix and column vector with all elements of 1, respectively. For a matrix L_1 , we let L_1^* denote its Hermitian matrix.

II. RELATED WORKS

A great deal of literature on the design of FDI attacks can be roughly divided into two categories, including designing the false data injection (FDI) attack signal [4], [15], [17]–[22] and the attack selection strategy [12]–[15].

FDI Attack Signal Design: The first fundamental work on launching the FDI attack signal is proposed by Liu *et al.* [4] in which the adversary could compromise measurements and change the results of state estimation without being detected by the bad measurement detection technique in smart grids. It reveals the potential secure breach of the power system when offline observations and system information are available to the adversary. Note that the design of the FDI attack signal depends on its attack objective and available information about the system model. In terms of the attack objective, the attack signal can be designed to maximize the remote state estimation error [18], the consensus error [15], the tracking error [23], and the quadratic cost function [17], to name a few. In view of the available information, the attack signal can be divided into two types, including model-based attack signal [18], [24] and data-driven one [20]–[22]. Among them, there are a large number of works on the optimal attack signal design. Nevertheless, few works focus on the property analysis of the optimal attack signal and explore the characteristic of the attack signal.

FDI Attack Selection Strategy: In [25], Pasqualetti *et al.* first studied the undetectable and unidentifiable FDI attack set where the adversary knows the full information about the system model and compromises sensors and actuators. It shows that the adversary has the ability to manipulate multiple attack objects without being detected. In the following, we review only works that are most pertinent to ours [12]–[15]. One type of work is to design switching attacks where the adversary can compromise only one agent at a time, which is basically considered as a kind of attack selection strategy. For example, Wu *et al.* [13] formulated an optimal switching attack design problem where the adversary aims to maximize the quadratic cost of states by determining the optimal compromised sensor sets. To relax the limitation on the number of compromised agents at a time, Luo *et al.* [15] proposed a submodularity-based FDI attack selection scheme where the adversary can manipulate multi-dimensional states for multiple agents. Nevertheless, note that the attack selection strategy is fixed and time-invariant. In practical scenarios, an intelligent adversary has the ability to change the subset of the compromised agents and dynamically adjust its attack selection strategy. For example, the substations can be compromised sequentially, whose combinations can cause severe large-scale outages in smart grids [7]. Hence, from the perspective of the adversary, it is promising and interesting to seek an efficient method to obtain a sequential attack selection strategy where the attack subset varies as the sequential sampling time, which is more practical and has better attack effects than the time-invariant attack selection strategy.

In a nutshell, different from separately handling the de-

sign of the attack signal and attack selection scheme, our work mainly centers on constructing the bridge between the attack signal and the attack selection strategy and tackling a sequential FDI attack co-design problem with these two coupled variables.

III. PROBLEM FORMULATION

A. System Model and Adversary Model

Consider a discrete-time dynamical system

$$x_{k+1} = A_k x_k + B_k u_k, \quad (1)$$

where $A_k \in \mathbb{R}^{n \times n}$, $B_k \in \mathbb{R}^{n \times m}$ are the system matrices, $x_k \in \mathbb{R}^n$ and $u_k \in \mathbb{R}^m$ are the system state and system input at time k , respectively. We set the linear feedback controller as $u_k = L_k x_k$. Then, we have

$$x_{k+1} = W_k x_k, \quad (2)$$

with the system matrix $W_k = A_k + B_k L_k$.

Consider an adversary can compromise system (1) by altering the original control law u_k or deviating the control signals from the true values, thus indirectly manipulating the system states x_k . For an adversary, it has the ability to flexibly select which agent to tamper with and design the injected attack signal simultaneously as time k varies. The dynamic system (2) under such attack can be remodeled as

$$x_{k+1}^a = W_k x_k^a + \Gamma_k \theta_k, \quad (3)$$

where $\theta_k \in \mathbb{R}$ is called *sequential* attack signal, the *sequential* attack selection strategy $\Gamma_k = [\gamma_k^1, \dots, \gamma_k^n]^T \in \mathbb{R}^n$ with the binary variable $\gamma_k^i = 1$ if the i -th agent is compromised at time k and $\gamma_k^i = 0$ otherwise. Then, we make the following assumption about the ability of the adversary and the definition of a sequential attack.

Assumption 1. *The adversary knows the exact knowledge of the system model.*

Assumption 1 is a common and implicit condition for the adversary to inject false data successfully [26].

Definition 1. (*Sequential attack*) *An attack is called sequential if it launches attack strategies (selects attack subsets or injects attack signals) as the sampling time k varies.*

B. Problem Formulation

In this work, we consider that the adversary's objective is to steer the system state to the expected malicious one as closely as possible in finite time by injecting the false data $\Gamma_k \theta_k$. The sum of the state error is characterized by J_1 , i.e.,

$$J_1 = \sum_{k=1}^N (\|x_k^a - x^*\|_{P_k}^2) + \|x_{N+1}^a - x^*\|_H^2,$$

where N is the given upper bound of finite-time iteration, x^* is the expected malicious state predefined by the adversary, and P_k and H are the positive definite weight matrices.

We also consider that the adversary desires to save the attack energy. The energy of injected false data is denoted as J_2 , i.e.,

$$J_2 = \sum_{k=0}^N (\|\Gamma_k \theta_k\|_{Q_k}^2),$$

where Q_k is the positive definite weight matrix.

Therefore, the total goal of the adversary is to reduce both the state error between the true system state and the expected malicious one and the consumed attack energy as much as possible. In N iterations, the injected false data includes the *sequential* attack signal $\theta \triangleq \{\theta_0, \theta_1, \dots, \theta_N\}$ and *sequential* attack selection strategy $\Gamma \triangleq \{\Gamma_0, \Gamma_1, \dots, \Gamma_N\}$. Under the injected false data, the sum of the state error and the consumed attack energy is expected to be minimized. To this end, constrained by the intrinsic system dynamic model (3), we construct the following optimization problem \mathcal{P}_0 .

$$\begin{aligned} \mathcal{P}_0 : \quad & \min_{\{\theta, \Gamma\}} J = J_1 + J_2 \\ & \text{s.t. } x_{k+1}^a = W_k x_k^a + \Gamma_k \theta_k. \end{aligned} \quad (4)$$

C. Problem Decomposition

The challenges of directly solving problem \mathcal{P}_0 result from the nonlinearity and non-convexity of the objective function J with respect to two closely coupled optimization variables Γ_k and θ_k . Furthermore, it is difficult to directly obtain the gradients of the objective function for variables θ and Γ to solve problem \mathcal{P}_0 . If we can explore the relationship between the attack signal θ_k and the attack selection strategy Γ_k and derive an analytical closed-form relation, it is vital to simplify the solution of problem \mathcal{P}_0 and reduce the difficulty of solving problem \mathcal{P}_0 . Concretely, we could first obtain the optimal attack signal when the attack selection strategy is given and known. Then we explore the feasible attack selection strategy based on the optimal attack signal in which there exists the relationship between the attack signal and the attack selection strategy. Thus, we decompose \mathcal{P}_0 into the following two sub-problems, i.e., problem \mathcal{P}_1 and \mathcal{P}_2 .

$$\begin{aligned} \mathcal{P}_1 : \quad & \min_{\{\theta_0, \theta_1, \dots, \theta_N\}} J = J_1 + J_2 \\ & \text{s.t. } x_{k+1}^a = W_k x_k^a + \Gamma_k \theta_k, \\ & \Gamma = \Gamma^\#, \end{aligned} \quad (5)$$

where the attack selection strategy $\Gamma^\#$ is given and known.

$$\begin{aligned} \mathcal{P}_2 : \quad & \min_{\{\Gamma_0, \Gamma_1, \dots, \Gamma_N\}} J = J_1 + J_2 \\ & \text{s.t. } x_{k+1}^a = W_k x_k^a + \Gamma_k \theta_k, \\ & \theta_k = \theta_k^\#, \end{aligned} \quad (6)$$

where $\theta_k^\#$ is obtained by solving problem \mathcal{P}_1 . The two sub-problems after decomposition are equivalent to the original problem since the multivariate optimization problem can be reduced to multiple univariate optimization problems if the closed-form analytical relationships among them are known.

To address problem \mathcal{P}_0 , we first focus on problem \mathcal{P}_1 . In problem \mathcal{P}_1 , we mainly analyze the relationship between the injected attack signal θ and the attack selection strategy

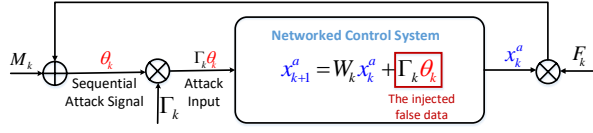


Fig. 1. The schematic of the optimal sequential attack signal design

Γ based on dynamic programming. Later, in Section V, we will deal with Γ with the heuristic learning-based algorithm under the obtained optimal *sequential* attack signal θ .

IV. OPTIMAL SEQUENTIAL ATTACK SIGNAL SCHEME

In this section, we solve problem \mathcal{P}_1 and derive the optimal sequential attack signal based on dynamic programming. Then, we excavate its critical parameters' property.

A. Optimal Attack Signal Design

Before demonstrating the sequential attack signal scheme, we introduce the notion of dynamic programming. Based on the Bellman principle of optimality, the key idea of dynamic programming is to transform the multi-stage decision problem to multiple single-stage decision problems. Concretely, if a multi-stage decision process satisfies the principle of optimality, it means that the decision sequence of the subsequent stages must be optimal for a state caused by the previous decision regardless of the initial state and the initial decision.

Motivated by the above observations, we aim to deal with problem \mathcal{P}_1 with dynamic programming. The schematic of the optimal sequential attack signal design is shown in Fig. 1, where the multi-time attack signal injection problem is transformed into multiple single-time attack signal injection problems. Specifically, given the attack selection strategy Γ_k , the critical parameters F_k and M_k can be obtained backward offline based on (8) and (10). Then, the solution of problem \mathcal{P}_1 , i.e., the optimal sequential attack signal θ_k is derived with the obtained F_k and M_k . The detailed solution is shown in the following theorem.

Theorem 1. (Optimal Sequential Attack Signal) *The optimal sequential attack signal θ_k for $k = 0, 1, \dots, N$, that minimizes J in (5) is*

$$\theta_k = F_k x_k^a + M_k, \quad (7)$$

where the critical parameter

$$F_k = -R_k^{-1} \Gamma_k^T K_{k+1} W_k, \quad (8)$$

with $R_k = \Gamma_k^T (Q_k + K_{k+1}) \Gamma_k$ and the intermediate variable

$$K_k = P_k + W_k^T K_{k+1} W_k + 2W_k^T K_{k+1} \Gamma_k F_k + F_k^T \Gamma_k^T (Q_k + K_{k+1}) \Gamma_k F_k, \quad (9)$$

and another critical parameter $M_k =$

$$\begin{cases} R_k^{-1} \Gamma_k^T K_{k+1} x^*, k = N, \\ R_k^{-1} \Gamma_k^T K_{k+1} (P_{k+1} x^* - W_{k+1}^T K_{k+2} \Gamma_{k+1} M_{k+1}), k \neq N. \end{cases} \quad (10)$$

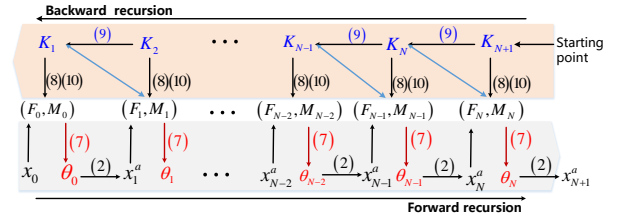


Fig. 2. The recursion flow of F_k , K_k , M_k and θ_k

Proof. The proof can be completed by solving the Bellman equation backward from time $N + 1$ of termination, shown in Appendix A. \square

Theorem 1 reveals the strongly coupled relationship between the optimal sequential attack signal and the attack selection strategy. Especially, the optimal attack signal θ_k at time k is the function of the system state x_k^a . Besides, it is related to the system structure W_k , the expected malicious state x^* , and the initial states x_0 . In other words, once the adversary knows the initial state x_0 and the system structure W_k , the optimal sequential attack signal θ_k can be designed after the adversary determines the expected malicious state x^* , the attack selection strategy Γ_k , and weight matrices P_k , Q_k and H . As shown in Fig. 2, with the initial matrix K_{N+1} , F_k , K_k and M_k are derived backward based on (8), (9) and (10), respectively. Then, with the known initial states x_0 and (7), the adversary can directly inject optimal sequential attack signal θ_k along the forward iteration timeline.

B. Property Analysis

In this part, we demonstrate the inverse convergence of the critical parameter matrix K_k in (9) and vector F_k in (8), respectively. Since K_k and F_k are derived backward, its inverse convergence is defined as follows.

Definition 2. (Inverse Convergence) *Matrix/Vector/Point convergence is called inverse convergence if the matrix/vector/point is derived backward and converges along the reverse order of iteration time.*

Based on Definition 2, we find that the sequential $\{K_N, K_{N-1}, K_{N-2}, \dots, K_2, K_1\}$ and $\{F_N, F_{N-1}, F_{N-2}, \dots, F_1, F_0\}$ converge forward, which are also called inverse convergence of K_k and F_k . With this property, it is possible to quickly obtain the steady-state parameters K_k and F_k . In other words, only a small number of iteration times k are required to derive F_k and K_k backward regardless of the finite-time N . Based on these few backward recursions, the optimal sequential attack signal can be directly designed.

In what follows, we first analyze the symmetry and positive definiteness of K_k , and the system's finite-time stability, which is beneficial to proving its inverse convergence.

Lemma 1 (Symmetry and positive definiteness of K_k). *The matrix K_k in (9) is a positive definite Hermitian matrix for $k = 0, 1, \dots, N$, i.e., $K_k = K_k^* \succ 0$.*

Proof. Please see Appendix B. \square

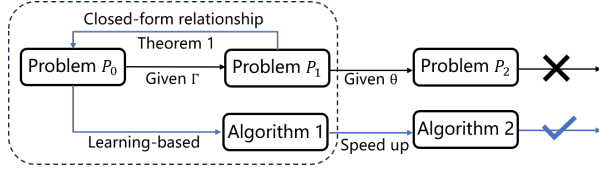


Fig. 3. The solving process of problem \mathcal{P}_0

Corollary 1. K_k in (9) can be simplified as

$$K_k = P_k + W_k^T K_{k+1} W_k - R_k^{-1} W_k^T K_{k+1} \Gamma_k \Gamma_k^T K_{k+1} W_k.$$

Combined with (9) and (27), the proof is completed.

Lemma 2 (Finite-time stability). *Consider a discrete-time system with a corresponding positive definite matrix-valued Lyapunov function $\tilde{V} : \mathbb{R}^{n \times n} \rightarrow \mathbb{R}$ and let $\tilde{V}_k = \tilde{V}(K_k - K^*)$. Let α and ϵ be a constant in the open interval $(0, 1)$. Let $\tilde{V}_N > 0$ be the finite initial value of the Lyapunov function with respect to K_k . Denote $\varphi_k \triangleq \varphi(\tilde{V}_k^{1-\alpha})$ where $\varphi : \mathbb{R}^+ \rightarrow \mathbb{R}^+$ is a class- \mathcal{K} function of $\tilde{V}_k^{1-\alpha}$ that satisfies*

$$\frac{\varphi_k}{\varphi_N} \geq 1 - \epsilon \quad \text{for} \quad \tilde{V}_k^{1-\alpha} \in (\tilde{V}_N^{1-\alpha} - \chi, \tilde{V}_N^{1-\alpha}) \quad (11)$$

for some finite positive constant $\chi < \tilde{V}_N^{1-\alpha}$. Then, if \tilde{V}_k satisfies the relation

$$\tilde{V}_{k-1} - \tilde{V}_k = -\varphi_k \tilde{V}_k^\alpha, \quad (12)$$

matrix K_k has the steady state and converges to K^* for $0 \leq k < \xi^*$ where the positive integer ξ^* satisfies (30).

Proof. The proof could be founded in Appendix C. \square

Lemma 2 provides a new insight to prove the finite-time inverse convergence for the matrix K_k in (9), which is also an extension of finite-time vector forward convergence [27] to matrix inverse convergence. Based on Lemma 2, then we develop a matrix-valued Lyapunov function in the following theorem to show the inverse convergence of K_k .

Theorem 2 (Finite-time inverse convergence of K_k). *Let ξ^* be the smallest integer for the inverse convergence of matrix K_k . The parameter matrix K_k in (9) converges inversely when $0 \leq k < \xi^*$ where ξ^* satisfies (30).*

Proof. The proof could be founded in Appendix D. \square

Corollary 2 (Inverse Convergence of F_k). *When the system structure W_k is fixed, the parameter vector F_k in (8) converges inversely when $0 \leq k < \xi^* + 1$.*

Proof. Since $F_k = -R_k^{-1} \Gamma_k^T K_{k+1} W_k$ with $R_k = \Gamma_k^T (Q_k + K_{k+1}) \Gamma_k$ and K_k in (9), the proof can be completed if the convergence of K_{k+1} is guaranteed. When $0 \leq k < \xi^*$, K_k converges inversely. Thus, F_k converges when $0 \leq k < \xi^* + 1$. The proof is completed. \square

V. LEARNING-BASED JOINT ATTACK STRATEGY

In this section, we propose a heuristic two-stage learning-based joint attack algorithm for solving problem \mathcal{P}_0 , whose idea is shown in Fig. 3. Concretely, we first obtain the optimal sequential attack signal when the attack selection strategy Γ is given, which is derived in Theorem 1 by addressing problem \mathcal{P}_1 . Note that computing θ_k necessitates knowledge of $\Gamma_k, \Gamma_{k+1}, \dots, \Gamma_N$ from Theorem 1, i.e.,

$$\theta_k = f(\Gamma_k, \Gamma_{k+1}, \dots, \Gamma_N), \quad (13)$$

where f is a function of Γ and characterizes the closed-form relation between the injected attack signal and the attack selection strategy, which is obtained by solving problem \mathcal{P}_1 . Then, with the prior relationship between Γ and θ in Theorem 1, we desire to deal with problem \mathcal{P}_2 . In essence, problem \mathcal{P}_2 is a multi-stage decision problem with 0-1 integer variables. The challenges of tackling problem \mathcal{P}_2 come from the 0-1 integer variables. It is difficult to directly obtain the analytical optimal solution of such a multi-stage 0-1 integer programming problem. Moreover, the size of the optimal sequential attack signal θ_k depends on the future attack selection strategy $\Gamma_k, \Gamma_{k+1}, \Gamma_{k+2}, \dots, \Gamma_N$, as shown in (7), making the problem more complicated to solve. A brute-force approach to solving this problem would result in an intractable exponential time complexity of $O(n^N)$.

To address the challenge of high time complexity, we employ a heuristic algorithm. Specifically, we use Reinforcement Learning (RL) approach, which shows great potential for handling optimization problems with sequential decision variables by leveraging the chronological information provided by a Markov Decision Process (MDP) approach. It is worth noting that for a problem to be cast as an MDP, it must satisfy the Markov condition, which stipulates that the transition and reward are contingent *solely* on the current situation [28], rather than on past or future states. However, the optimal sequential attack signal θ_k in (7) cannot be directly derived based on the given attack selection strategy Γ_k , i.e., *problem \mathcal{P}_2 cannot be modeled as an MDP process*. How to tackle the dependency relationship between θ_k and $\Gamma_k, \Gamma_{k+1}, \dots, \Gamma_N$ is critical for designing a feasible scheme to obtain the multi-stage attack selection strategy.

To circumvent this issue and ensure the Markov property is maintained, we recall problem \mathcal{P}_0 , in which we add the constraint (13) and the speciality is to exploit the actual optimal attack signal θ_k^* derived in (7) as the prior knowledge and introduce a penalty term in the computation of the reward function. The solving procedure for this problem \mathcal{P}_0 will be elaborated in the subsequent subsections.

$$\begin{aligned} \mathcal{P}_0 : \quad & \min_{\{\Gamma, \theta\}} J = J_1 + J_2 & (14) \\ \text{s.t.} \quad & x_{k+1}^a = W_k x_k^a + \Gamma_k \theta_k, \\ & \theta_k^* = f(\Gamma_k, \Gamma_{k+1}, \dots, \Gamma_N), \forall k. \end{aligned}$$

Here, ϕ is a constant weight coefficient.

A. Problem \mathcal{P}_0 Remodeling

First, we consider a finite-horizon discounted Markov decision process (MDP) to directly solve problem \mathcal{P}_0 in (14), which is defined as $\mathcal{M} = (\mathcal{S}, \mathcal{A}, P, N, r, \gamma)$ below:

- 1) System States Space $\mathcal{S} = \{x_k^a\}$: The system state under the optimal sequential attack at time k is designed as $x_k^a = [x_k^{\{a,1\}}, x_k^{\{a,2\}}, \dots, x_k^{\{a,n\}}]^T$, where $x_k^{\{a,i\}} \in \mathbb{R}$ is the state of the i -th agent under attacks.
- 2) Action Space $\mathcal{A} = \{\Gamma, \theta\}$: Action space consists of the attack selection decision Γ and the attack signal θ . A binary attack selection vector $\Gamma_k = [\gamma_k^1, \gamma_k^2, \dots, \gamma_k^n]^T$ is used to denote the attack selection decision at time k with $\gamma_k^i \in \{0, 1\}$. If $\gamma_k^i = 1$, then the i -th agent is selected to be compromised at time k , otherwise $\gamma_k^i = 0$. The attack signal $\theta_k \in \mathbb{R}$ is applied for compromising states at time k .
- 3) System Dynamics P : With the given state x_k^a , the attack selection decision Γ_k and the attack signal θ_k , the dynamics of the state are depicted as (3), namely

$$x_{k+1}^a = W_k x_k^a + \Gamma_k \theta_k.$$

- 4) Reward function $r : \mathcal{S} \times \mathcal{A} \rightarrow \mathbb{R}$: We adopt the objective function in (14) to design the one-step reward function

$$r_k(x_k^a, \Gamma_k, \theta_k | x^*, \theta_k^*) = - \|x_{k+1}^a - x^*\|_{P_k}^2 - \|\Gamma_k \theta_k\|_{Q_k}^2 - \phi(\theta_k - \theta_k^*)^2. \quad (15)$$

- 5) Constants: $N \in \mathbb{R}$ is the horizon (episode length) and $\gamma \in (0, 1)$ is the discount factor.

Our goal is to find a stochastic policy $\pi : \mathcal{S} \rightarrow \mathcal{A}$. With the given state x_k^a , the policy decides what action Γ_k, θ_k to take. Concretely, the objective of the adversary is to find a good policy π to maximize the expected discounted total reward, given by

$$\mathbb{E}_\pi \left[\sum_{k=0}^{N-1} \gamma^k r_k(x_k^a, \Gamma_k, \theta_k | x^*, \theta_k^*) \right]. \quad (16)$$

B. Learning-based Joint Attack Strategy Design

Policy-based algorithms have achieved great success in solving complicated dynamic problems [30], [31], enjoying good sample efficiency. The key idea of the policy-based algorithms is to increase the probability of the actions leading to higher rewards. We propose a learning-based algorithm (Algorithm 1) that utilizes our prior knowledge about the relationship between the attack selection strategy and the attack signal in (13). We initialize a random policy π_0 and follow the steps below to update the policy π_t iteratively. Our algorithm cycles through three phases, described below.

- 1) Data collection (Line 4-10): Initialize the environment state as x_0^a and the buffer $\mathcal{B} = \emptyset$. The agent interacts with the environment by taking actions $\{\Gamma_k, \theta_k\}$ sampling from the current policy $\pi_t(x_k^a)$. The environment then updates the state according to the dynamic function to attain $x_{k+1}^a = P(x_k^a, \Gamma_k, \theta_k)$. Store the data

Algorithm 1: One-stage Learning-based Algorithm

Input: The expected malicious state x^* ; the initial state x_0 ; episode length N ; stopping criterion δ ; data buffer \mathcal{B}

Output: A trained policy π^*

- 1 Initialize the policy π , last performance $J_l = 0$, current performance $J_c = 0$
- 2 **while** $J_c - J_l < \delta$ **do**
- 3 $J_l = J_c$;
- 4 Initialize the x_0 , buffer $\mathcal{B} = \emptyset$;
- 5 // data collection
- 6 **for** $k = 0, 1, 2, \dots, N$ **do**
- 7 $\Gamma_k, \theta_k = \pi(x_k^a)$; // Decision procedure
- 8 $x_{k+1}^a = W_k x_k^a + \Gamma_k \theta_k$; // Model dynamic (3)
- 9 $\mathcal{B} \leftarrow \mathcal{B} \cup \{x_k^a, \Gamma_k, \theta_k\}$; // Store data
- 10 **end**
- 11 // computing rewards
- 12 **for** $k = 0, 1, 2, \dots, N$ **do**
- 13 Compute θ_k^* as described in Fig. 2.
- 14 // adopting (13) to compute θ_k^*
- 15 $r_k = R(x_k^a, \Gamma_k, \theta_k | x^*, \theta_k^*)$; // Reward function (15)
- 16 Substitute $(x_k^a, \Gamma_k, \theta_k)$ with $(x_k^a, \Gamma_k, \theta_k, r_k)$ in \mathcal{B} .
- 17 **end**
- 18 Compute the current performance $J_c = J$
- 19 // model training
- 20 Train the policy π with data in \mathcal{B} using PPO; See details in [29].
- 21 **end**
- 22 **return** $\pi^* = \pi$

in the buffer \mathcal{B} . It moves to the next phase when an episode ends (when $k > N$).

- 2) Reward computation (Line 11-17): The data in the data buffer \mathcal{B} do not have the reward information because computing the reward in (13) requires the optimal sequential attack signal θ^* which needs complete knowledge of the sequential attack selection strategy Γ . Thus, the optimal sequential attack signal can only be attained after a complete episode. We first compute the $\theta_0^*, \dots, \theta_{N-1}^*, \theta_N^*$ with our methods described in Fig. 2. Then, we can compute the reward r_k with (15) using $(x_k^a, \Gamma_k, \theta_k, \theta_k^*)$. At last, we store the reward into the buffer \mathcal{B} by substituting $(x_k^a, \Gamma_k, \theta_k)$ with $(x_k^a, \Gamma_k, \theta_k, r_k)$.
- 3) Policy training (Line 19-20): Now we have a buffer $\mathcal{B} = \{(x_k^a, \Gamma_k, \theta_k, r_k)\}$, which contains the state-action-reward tuple. With this buffer, we update the policy parameters adopting the Proximal Policy Optimization (PPO) algorithm, described in [29].

We repeat these three phases until the policy is converged where the parameter δ is set as small as possible. The convergence of the obtained solution of PPO is discussed in [32]. When we assume $n = 3$ and $N = 50$, directly

Algorithm 2: Heuristic Two-stage Learning-based Joint Attack Algorithm (HTL-JA)

Input: The expected malicious state x^* ; the initial state x_0 ; the number of trajectory T_r .

Output: Sequential attack selection strategy Γ and sequential attack signal θ .

- 1 **Stage 1:** Attain a sub-optimal policy π under Algorithm 1 with a loose stopping criterion;
 - 2 **Stage 2:** Generate T_r alternative attack strategies $\{(\Gamma^{(1)}, \theta^{(1)}), \dots, (\Gamma^{(T_r)}, \theta^{(T_r)})\}$ based on π ;
 - 3 Initialize best strategy $BS = \emptyset$; current min objective $J^* = \infty$;
 - 4 **for** $i = 1, 2, \dots, T_r$ **do**
 - 5 Compute the optimal sequential attack signal $\theta^{*(i)}$ given $\Gamma^{(i)}$ based on Theorem 1;
 - 6 **if** $J(\Gamma^{(i)}, \theta^{*(i)}) < J^*$ **then**
 - 7 $BS \leftarrow (\Gamma^{(i)}, \theta^{*(i)})$;
 - 8 $J^* \leftarrow J(\Gamma^{(i)}, \theta^{*(i)})$;
 - 9 **end**
 - 10 **end**
 - 11 **return** BS ;
-

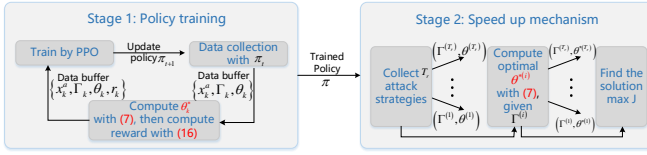


Fig. 4. The schematic of Algorithm 2 (HTL-JA)

applying Algorithm 1 to solve problem \mathcal{P}_0 in (14) would reach the optimal performance of the objective function value $J = 30$ with 4.1×10^4 samples, which is much less than the brute-force approach with $2^{3^{50}} \approx 1.4 \times 10^{45}$ samples, as demonstrated in Table IV of Section VI-B.

C. A Two-stage Mechanism to Speed Up

Algorithm 1 is referred to one-stage learning-based algorithm. Note that the convergence procedure of Algorithm 1 suffers from a long tail effect: the objective function reaches the sub-optimal very quickly, but it takes multiple times of epochs to reach the optimal value. Thus, we utilize our system knowledge to propose a two-stage learning-based algorithm to tackle this problem and find an approximate solution with much less consumption, as shown in Algorithm 2. The stage 1 depends on Algorithm 1 and is almost exactly the same as Algorithm 1 except the setting of the parameter δ . In stage 1, δ is set to be larger than that in Algorithm 1 since we aim to achieve a sub-optimal policy π rather than attain the optimal converged policy in Algorithm 1. In stage 2, with the sub-optimal policy π , the agent generates several alternative sequential attack selection sequences $\{\Gamma^{(1)}, \dots, \Gamma^{(T_r)}\}$ where T_r is the number of the sequential attack selection strategies. Then we traverse all the alternative sequential attack selection strategies to compute

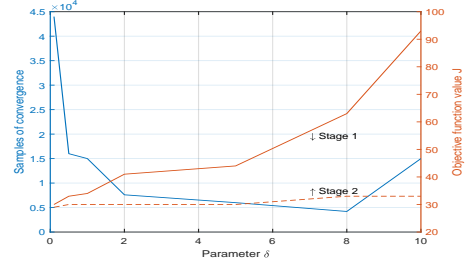


Fig. 5. The effects of δ on samples and objective function value

corresponding theoretically optimal sequential attack signals $\{\theta^{*(1)}, \dots, \theta^{*(T_r)}\}$ based on Theorem 1. The following lemma is provided to show the feasibility of the obtained solution in step 6-10 of Algorithm 2.

Lemma 3. *With the optimal sequential attack signal $\theta^{*(i)}$ in Theorem 1, we have*

$$J(\Gamma^{(i)}, \theta^{*(i)}) \leq J(\Gamma^{(i)}, \theta^{(i)}), \quad (17)$$

for any $i \in \{1, 2, \dots, T_r\}$.

Proof. Since $\theta^{*(i)}$ is the optimal solution of problem \mathcal{P}_1 , (17) can be directly validated under the given attack selection strategy $\Gamma^{(i)}$. \square

In a word, the two-stage learning-based attack framework is provided in Fig. 4, where the trained sub-optimal policy π^* in stage 1 paves way to speed up the procedure of reaching the optimal solution of problem \mathcal{P}_0 in stage 2.

Remark 1 (Parameter δ). *To deepen our understanding of δ , herein we discuss the effects of the parameter δ on the proposed one-stage and two-stage learning-based algorithms. Note that the difference between Algorithm 1 and stage 1 in Algorithm 2 lies in the parameter δ . When δ approaches zero, stage 1 in Algorithm 2 is the same as Algorithm 1. Consider a consensus process with three agents, shown in Section VI. The relationship among δ , the samples of convergence and the objective function value J is depicted in Fig. 5. When δ approaches zero, we find that the samples of convergence increases rapidly. In other words, Algorithm 1 needs large number of samples to obtain the feasible solution than Algorithm 2. When $\delta = 8$, the proposed algorithms do not reach the minimum objective function value while keeping the minimum samples. In addition, it illustrates that the two-stage learning mechanism plays an important role in accelerating the convergence process and the objective function value J will converge to 30 and decreases as δ approaches zero.*

Remark 2 (Optimality). *Note that the policy gradient optimization method is the basis of the proposed heuristic two-stage learning-based algorithm. Hence, the optimality of the proposed algorithm also depends on that of the policy gradient method, whose convergence and optimality are analyzed in [33, Theorem 5]. We find that the lower bound of the optimality error between the objective function value under the optimal solution and that under the actual*

solution is less than required bound ε . Concretely, the bound ε is proportional to the dimensions of states and the discount factor γ , and inversely proportional to iterations T . In addition, in [34], the upper bound of the global optimality of stationary point is demonstrated. Both works provide the feasible analysis for the convergence and optimality of the policy gradient method, thus showing the potential insights to guarantee the convergence and optimality of the proposed algorithm, which deserves further investigation in the future.

VI. SIMULATION RESULTS

In this section, we evaluate the performance of the optimal sequential attack signal and attack selection strategy, respectively.

A. Performance of Optimal Sequential Attack Signal

In this part, we analyze the driving performance of the obtained sequential attack signal and the inverse convergence of its critical parameters K_k and F_k .

Consider a consensus process with three agents where the dynamics of the whole system satisfy (1). We set the matrix $W = I_3 - 0.2 * L$, which can achieve the average consensus without attacks. Meanwhile, the system is stable and controllable. In the linear network, the Laplacian matrix $L = [1 \ -1 \ 0; -1 \ 2 \ -1; 0 \ -1 \ 1]$ and $L = [2 \ -1 \ -1; -1 \ 2 \ -1; -1 \ -1 \ 2]$ in the circle network. Let time $N = 50$, and weight matrices $P_k = Q_k = H = I_3$ for all $0 \leq k \leq N$. Then we set the critical parameter $K_{N+1} = H$, the initial state $x_0 = [-1 \ 12 \ -5]^T$ and the expected malicious state $x^* = [0 \ 0 \ 0]^T$.

1) *Effects of the sequential attack signal θ on the system states:* Given the attack selection strategy $\Gamma_1 = [1 \ 0 \ 0]^T$ and the linear network, the differences between the states without attacks and that with the injected attack signal θ are shown in Fig. 6(a). It is illustrated that the injected sequential attack signal can steer the average consensus value $[2 \ 2 \ 2]^T$ to the desired malicious state $x^* = [0 \ 0 \ 0]^T$.

2) *Effects of the attack selection strategy Γ on θ under different networks:* We set attack selection strategy $\Gamma_1 = [1 \ 0 \ 0]^T$, $\Gamma_2 = [0 \ 1 \ 0]^T$, and $\Gamma_3 = [0 \ 0 \ 1]^T$. The effects of different attack selection strategies on the injected sequential attack signal under linear and cycle networks are shown in Fig. 6(b). Notably, the injected attack signal θ varies with the distinct attack selection strategies and approaches zero. Moreover, from Table I and Table II, we find that there exists a trade-off between the injected attack energy and the objective function value regardless of the type of connected networks. Specifically, the more the objective function needs to be minimized while driving the states to the malicious states, the more attack energy needs to be injected.

3) *Effects of the initial states on θ :* We set two types of initial states $x_0^{(1)} = [-1 \ 12 \ -5]^T$ and $x_0^{(2)} = [-1 \ 10 \ -15]^T$, and remain the other conditions. The effects of the initial states on the injected optimal sequential attack signal θ are shown in Fig. 6(c). It is illustrated that the size of the

TABLE I
RESULTS OF DIFFERENT ATTACK SELECTION IN LINEAR NETWORKS

Network structure	Attack selection strategy Γ	Attack energy $\sum_{k=0}^N \ \Gamma_k \theta_k\ ^2$	Objective J
Linear	$[1 \ 0 \ 0]^T$	6.8787	68.6639
	$[0 \ 1 \ 0]^T$	14.7073	36.0239
	$[0 \ 0 \ 1]^T$	3.0517	130.6101

TABLE II
RESULTS OF DIFFERENT ATTACK SELECTION IN CIRCLE NETWORKS

Network structure	Attack selection strategy Γ	Attack energy $\sum_{k=0}^N \ \Gamma_k \theta_k\ ^2$	Objective J
Circle	$[1 \ 0 \ 0]^T$	5.9828	64.0186
	$[0 \ 1 \ 0]^T$	14.7073	23.3255
	$[0 \ 0 \ 1]^T$	4.9348	72.1756

injected attack signal highly depends on the initial states. Even though there exists the same initial state for agent 1, the size of the injected attack signal is different and influenced by the initial states of other agents.

4) *Inverse convergence of K_k and F_k :* In this part, we show the inverse convergence of K_k and F_k , which are measured by the following index $K_c \triangleq \|K_k - K^*\|$ and $F_c \triangleq \|F_k - F^*\|$, where K^* and F^* are the steady-state matrix of K_k and F_k for $0 \leq k \leq N$, respectively. Given the attack selection strategy $\Gamma_1 = [1 \ 0 \ 0]^T$ and the other same conditions as the first part, the convergence error of K_k and F_k are illustrated as Fig. 7(a) and Fig. 7(b). Under the linear network, when the first or the third agent is compromised, the convergence error of K_k and F_k are the same, which is different from that when the only second agent is attacked. In other words, the effects of attack selection strategies on the injected attack signal depend on the network structure. Especially, under the cycle network, the selection of the compromised agents does not affect the injected signal. Moreover, comparing Fig. 7(a) with Fig. 7(b), it is easy to reveal that the convergence rate of F_k is greater than that of K_k , which is owing to the convergence of weight matrix W_k . From Table III, we show the inverse convergence times for K_k and F_k , which validate the result in Corollary 2. Meanwhile, we find that only 15 iteration times are required to compute K_k and 14 iteration times for F_k regardless of the length of N .

TABLE III
TIMES OF INVERSE CONVERGENCE OF K_k AND F_k

Length of N	50	100	200	1000
Inverse Convergence Time of K_k	[1, 35]	[1, 85]	[1, 185]	[1, 985]
Inverse Convergence Time of F_k	[1, 36]	[1, 86]	[1, 186]	[1, 186]

B. Performance of Learning-based Attack Selection Strategy

1) *Parameter setting:* Consider the aforementioned consensus process with three agents and the same parameter

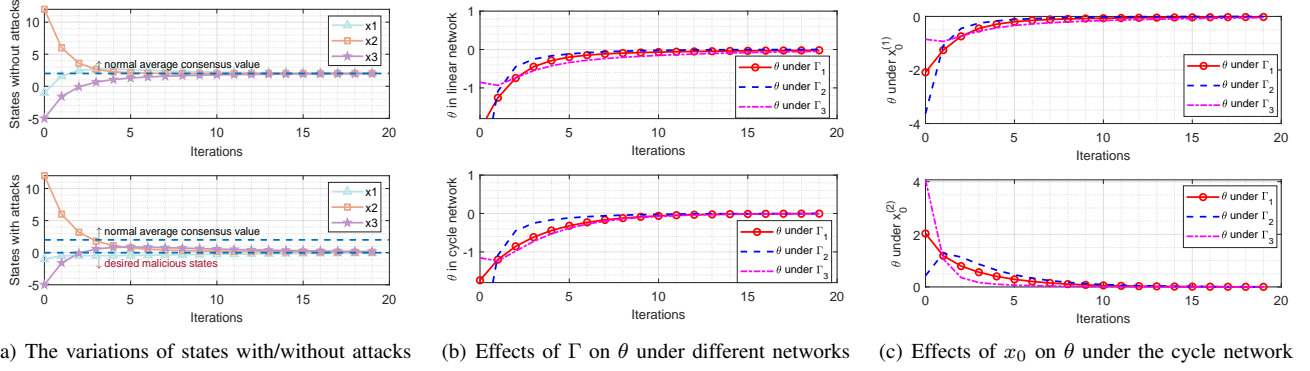


Fig. 6. Performance of the optimal sequential attack signal.

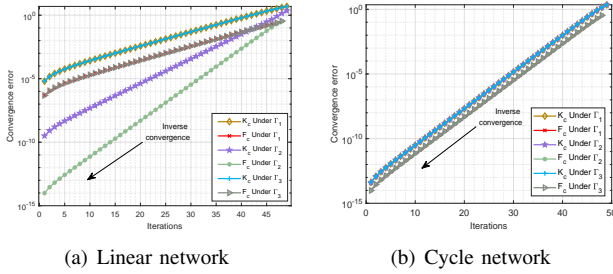


Fig. 7. The convergence error of K_k and F_k under different networks.

settings. Meanwhile, the stopping criterion δ in Algorithm 1 and the number of trajectory T_r in Algorithm 2 are set as $\delta = 2$ and $T_r = 10$, respectively. In addition, we consider the consensus process with ten agents where the Laplacian matrix is designed as $L = [2 \ -1 \ 0 \ 0 \ 0 \ 0 \ 0 \ 0 \ -1; -1 \ 3 \ -1 \ -1 \ 0 \ 0 \ 0 \ 0 \ 0; 0 \ -1 \ 2 \ 0 \ 0 \ -1 \ 0 \ 0 \ 0; 0 \ -1 \ 0 \ 3 \ -1 \ -1 \ 0 \ 0 \ 0; 0 \ 0 \ -1 \ 1 \ 0 \ 0 \ 0 \ 0 \ 0; 0 \ 0 \ 0 \ -1 \ 0 \ 2 \ 0 \ 0 \ -1 \ 0; 0 \ 0 \ -1 \ 0 \ 0 \ 2 \ -1 \ 0 \ 0; 0 \ 0 \ 0 \ 0 \ 0 \ -1 \ 2 \ -1 \ 0; 0 \ 0 \ 0 \ 0 \ 0 \ -1 \ 0 \ -1 \ 2 \ 0; -1 \ 0 \ 0 \ 0 \ 0 \ 0 \ 0 \ 0 \ 0 \ 1]$, and the initial state is set as $x_0 = [-1, 12, -5, 5, 2, 7, 7, 0, 9, -10]^T$. We remain the other conditions and set $\delta = 0.1$ for Algorithm 1 and $\delta = 2$ for Algorithm 2.

2) *Compared algorithms*: In this part, we compare five kinds of algorithms. The first approach is the brute force method. The second approach is the random selection strategy, where both the sequential attack selection strategy Γ and the attack signal θ are randomly generated. The third approach is the sampling-based algorithm where Γ is randomly sampled and exploited to compute θ based on Theorem 1, generating the optimal strategy after multiple samples. The fourth approach is to apply Algorithm 1 to obtain the solution of the attack selection strategy and the injected attack signal, respectively. The fifth approach is our algorithm, i.e., Algorithm 2, where the prior information about the attack signal in (7) is used to evaluate and the two-stage learning-based mechanism is adopted to speed up the convergence process.

3) *Results*: As depicted in Fig. 8, we need more than 4.1×10^4 samples if Algorithm 1 is desired to converge to the optimal solution ($J \approx 30$). However, if we adopt the

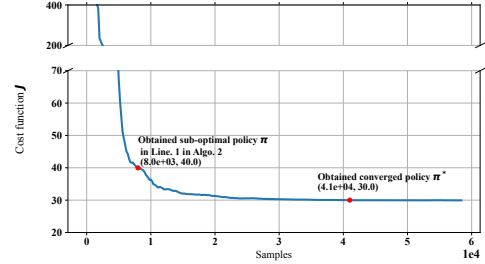


Fig. 8. The result of learning-based algorithms

two-stage mechanism, we can jump out the RL iteration at a sub-optimal solution ($J \approx 40$) and refine it with our stage 2 in Algorithm 2 to reach $J = 30$. This means that we can reach the optimal solution with only 8.0×10^3 samples, much less than the one-stage learning-based algorithm (Algorithm 1). The result of comparison among several algorithms is shown in Table IV. Note that the sampling-based selection strategy seems better than the proposed algorithm under the three agents. Probably because the number of agents is too small, the considered scenario is simple and easy to obtain the optimal solution based on the random sampling. When ten agents are considered, Table IV further validates the conjecture since the sampling-based strategy does not work well. We find that the effectiveness of the proposed algorithm is not affected by the number of agents. Algorithm 2 can reach the optimal objective function value with the minimum samples compared to Algorithm 1. Meanwhile, compared with the sampling-based strategy, Algorithm 2 obtains lower objective function value while the time complexity is low.

VII. CONCLUSION

We constructed an optimal sequential false data injection attack co-design framework where the injected attack signals and attack selection strategy are strongly coupled optimization variables and vary with the sampling time in discrete-time systems. Specifically, we first derived an optimal sequential attack signal, which showcases the closed-form explicit expression between the injected attack signal and the attack selection strategy. In addition, we proved the inverse convergence of the critical parameters in the optimal sequential attack signal. Furthermore, with the prior

TABLE IV
COMPARISONS OF ALGORITHMS UNDER DIFFERENT AMOUNT OF AGENTS

#Agents	THREE		TEN	
Algorithms	Time Complexity (Sample Size) ↓	J ↓	Time Complexity ↓	J ↓
Brute force	1.4×10^{45}	N/A	1.0×10^{53}	N/A
Random	1.0×10^6	4039	1.0×10^6	21311
Sampling-based	1.0×10^5	27.8	1.0×10^5	318.0
Algorithm 1	4.1×10^4	30.0	5.1×10^4	295.0
Algorithm 2	8.0×10^3	30.0	1.8×10^4	295.0

knowledge of the closed-form relationship, we proposed the heuristic learning-based attack algorithms to obtain the sequential feasible solution. Future work will strive to design the resilient algorithms to defend the system against the proposed optimal sequential FDI attacks.

APPENDIX

A. Proof of Theorem 1

The proof can be completed by solving the Bellman equation backward from time $N + 1$ of termination.

When time $k = N + 1$, $K_{N+1} = H$, for any $x_{N+1}^a \in \mathbb{R}^n$, the value function

$$\begin{aligned} V(x_{N+1}^a, N + 1) &= (x_{N+1}^a - x^*)^T H (x_{N+1}^a - x^*) \\ &= (x_{N+1}^a)^T K_{N+1} (x_{N+1}^a) + G_{N+1}, \end{aligned} \quad (18)$$

where $G_{N+1} = -2(x_{N+1}^a)^T K_{N+1} x^* + \|x^*\|^2$. Note that the value function $V(x_{N+1}^a, N + 1)$ is the quadratic function with respect to x_{N+1}^a . Next, with the mathematical induction method, we prove that the value function always satisfies the following form

$$V(x_{k+1}^a, k + 1) = (x_{k+1}^a)^T K_{k+1} (x_{k+1}^a) + G_{k+1}, \quad (19)$$

where K_{k+1} is the real symmetric positive definite matrix for $k = 0, 1, \dots, N$.

Then, we derive the optimal attack signal θ_N at time N . With the obtained value function $V(x_{N+1}^a, N + 1)$ in (18), for any $x_N^a \in \mathbb{R}^n$, we have

$$\begin{aligned} V(x_N^a, N) &= \min_{\theta_N} \left\{ (x_N^a - x^*)^T P_N (x_N^a - x^*) \right. \\ &\quad \left. + \|\Gamma_N \theta_N\|_{Q_N}^2 + V(x_{N+1}^a, N + 1) \right\} \\ &= \min_{\theta_N} \left\{ (x_N^a - x^*)^T P_N (x_N^a - x^*) \right. \\ &\quad \left. + (W_N x_N^a + \Gamma_N \theta_N)^T K_{N+1} (W_N x_N^a + \Gamma_N \theta_N) \right. \\ &\quad \left. + \theta_N^T \Gamma_N^T Q_N \Gamma_N \theta_N + G_{N+1} \right\}. \end{aligned} \quad (20)$$

Taking the derivative of (20) with respect to θ_N , for any $x_N^a \in \mathbb{R}^n$, we have $2\theta_N^T \Gamma_N^T Q_N \Gamma_N + 2(W_N x_N^a + \Gamma_N \theta_N)^T K_{N+1} \Gamma_N = 0$. Thus, it can be inferred that

$$\theta_N = -R_N^{-1} (\Gamma_N^T K_{N+1} W_N x_N^a - \Gamma_N^T K_{N+1} x^*), \quad (21)$$

where $R_N \triangleq \Gamma_N^T (Q_N + K_{N+1}) \Gamma_N$. (21) is rewritten as

$$\theta_N = F_N x_N^a + M_N, \quad (22)$$

where $F_N = -[\Gamma_N^T (Q_N + K_{N+1}) \Gamma_N]^{-1} \Gamma_N^T K_{N+1} W_N$ and $M_N = [\Gamma_N^T (Q_N + K_{N+1}) \Gamma_N]^{-1} \Gamma_N^T K_{N+1} x^*$.

When time $k = N$, combined with (20) and (22), we derive the value function

$$\begin{aligned} V(x_N^a, N) &= (x_N^a)^T \left\{ P_k + W_k^T K_{k+1} W_k + 2W_k^T K_{k+1} \Gamma_k F_k \right. \\ &\quad \left. + F_k^T \Gamma_k^T (Q_k + K_{k+1}) \Gamma_k F_k \right\} (x_N^a) + G_{N+1} \\ &\quad - 2(x^*)^T P_N x_N^a + \|x^*\|^2 \\ &\quad + \theta_N^T \Gamma_N^T (Q_N + K_{N+1}) \Gamma_N \theta_N \\ &\quad + 2x_N^T W_N^T K_{N+1} \Gamma_N M_N. \end{aligned} \quad (23)$$

Let

$$\begin{aligned} K_N &\triangleq P_N + W_N^T K_{N+1} W_N + 2W_N^T K_{N+1} \Gamma_N F_N \\ &\quad + F_N^T \Gamma_N^T (Q_N + K_{N+1}) \Gamma_N F_N \end{aligned}$$

and

$$\begin{aligned} G_N &\triangleq G_{N+1} - 2(x^*)^T P_N x_N^a + 2x_N^T W_N^T K_{N+1} \Gamma_N M_N \\ &\quad + \theta_N^T \Gamma_N^T (Q_N + K_{N+1}) \Gamma_N \theta_N + \|x^*\|^2. \end{aligned}$$

Thus, the value function $V(x_N^a, N)$ also satisfies (19).

Then, we derive the optimal attack signal θ_{N-1} at time $N - 1$. With the obtained value function $V(x_N^a, N)$ in (20), for any $x_{N-1}^a \in \mathbb{R}^n$, we have

$$\begin{aligned} V(x_{N-1}^a, N - 1) &= \min_{\theta_{N-1}} \left\{ (x_{N-1}^a - x^*)^T P_{N-1} (x_{N-1}^a - x^*) \right. \\ &\quad \left. + \|\Gamma_{N-1} \theta_{N-1}\|_{Q_{N-1}}^2 + V(x_N^a, N) \right\} \\ &= \min_{\theta_{N-1}} \left\{ (x_{N-1}^a - x^*)^T P_{N-1} (x_{N-1}^a - x^*) \right. \\ &\quad \left. + \theta_{N-1}^T \Gamma_{N-1}^T Q_{N-1} \Gamma_{N-1} \theta_{N-1} \right. \\ &\quad \left. + (W_{N-1} x_{N-1}^a + \Gamma_{N-1} \theta_{N-1})^T \right. \\ &\quad \left. K_N (W_N x_{N-1}^a + \Gamma_N \theta_{N-1}) + G_N \right\}. \end{aligned} \quad (24)$$

Taking the derivative of (24) with respect to θ_{N-1} , for any $x_{N-1}^a \in \mathbb{R}^n$, we have $2\theta_{N-1}^T \Gamma_{N-1}^T Q_{N-1} \Gamma_{N-1} + 2(W_{N-1} x_{N-1}^a + \Gamma_{N-1} \theta_{N-1})^T K_N \Gamma_{N-1} = 0$. Thus, it can be inferred that

$$\begin{aligned} \theta_{N-1} &= -R_{N-1}^{-1} (\Gamma_{N-1}^T K_N W_{N-1} x_{N-1}^a \\ &\quad - \Gamma_{N-1}^T K_N P_N x^* + W_{N-1}^T K_{N+1} \Gamma_N M_N), \end{aligned} \quad (25)$$

which also can be derived as $\theta_{N-1} = F_{N-1} x_{N-1}^a + M_{N-1}$ with $F_{N-1} = -R_{N-1}^{-1} \Gamma_{N-1}^T K_N W_{N-1}$ and

$$M_{N-1} = R_{N-1}^{-1} \Gamma_{N-1}^T K_N (P_N x^* - W_{N-1}^T K_{N+1} \Gamma_N M_N).$$

When time $k = N - 1$, combined (24) with (25), we derive the value function

$$V(x_{N-1}^a, N - 1) = (x_{N-1}^a)^T K_{N-1} (x_{N-1}^a) + G_{N-1},$$

where

$$\begin{aligned} K_{N-1} &= P_{N-1} + W_{N-1}^T K_N W_{N-1} + 2W_{N-1}^T K_N \Gamma_{N-1} F_{N-1} \\ &\quad + F_{N-1}^T \Gamma_{N-1}^T (Q_{N-1} + K_N) \Gamma_{N-1} F_{N-1} \end{aligned}$$

and

$$\begin{aligned}
G_{N-1} &= G_N - 2(x^*)^T P_{N-1} x_{N-1}^a \\
&\quad + \|x^*\|^2 + \theta_{N-1}^T \Gamma_{N-1}^T (Q_{N-1} + K_N) \Gamma_{N-1} \theta_{N-1} \\
&\quad + 2x_{N-1}^T W_{N-1}^T K_N \Gamma_{N-1} M_{N-1}.
\end{aligned}$$

Continue the iterative process for $k = 0, 1, \dots, N-2$. Finally, we can obtain the optimal sequential attack signal

$$\theta_k = F_k x_k^a + M_k,$$

and the value function

$$V(x_{k+1}^a, k+1) = (x_{k+1}^a)^T K_{k+1} x_{k+1}^a + G_{k+1},$$

Thus, the proof is completed.

B. Proof of Lemma 1

The proof can be divided into two parts. One is to show the Hermitian matrix K_k . The other is to show $K_k \succ 0$. Both are based on the mathematical induction method.

Hermitian. Let $P_k = Q_k = H_k = I$ for $k = 0, 1, \dots, N$. Since W_k is a real symmetrical matrix, we have $W_k = W_k^*$. When $k = N$, we have $K_{N+1} = I$, which is a real symmetrical matrix. We assume that K_1 is a real symmetrical matrix. Then when $k = 0$, it holds that

$$\begin{aligned}
K_0 &= P_0 + W_0^T K_1 W_0 + 2W_0^T K_1 \Gamma_0 F_0 \\
&\quad + F_0^T \Gamma_0^T (Q_0 + K_1) \Gamma_0 F_0.
\end{aligned} \tag{26}$$

Since $F_0 = -R_0^{-1} \Gamma_0^T K_1 W_0$ is a real matrix with $R_0 = \Gamma_0^T (Q_0 + K_1) \Gamma_0 = R_0^*$, then it can be inferred that

$$\begin{aligned}
K_0^* &= P_0^* + W_0^* K_1 W_0 + F_0^* \Gamma_0^* (Q_0 + K_1) \Gamma_0 F_0 \\
&\quad + 2F_0^* \Gamma_0^* K_1 W_0 \\
&= P_0 + W_0 K_1 W_0 + F_0^T \Gamma_0^T (Q_0 + K_1) \Gamma_0 F_0 \\
&\quad - 2W_0^* K_1 \Gamma_0 R_0^{-1} \Gamma_0^* K_1 W_0 \\
&= P_0 + W_0 K_1 W_0 + F_0^T \Gamma_0^T (Q_0 + K_1) \Gamma_0 F_0 \\
&\quad - 2W_0^T K_1 \Gamma_0 R_0^{-1} \Gamma_0^T K_1 W_0 \\
&= K_0.
\end{aligned}$$

Thus, K_0 is also a real symmetrical matrix. In summary, K_k is a Hermitian matrix for $k = 0, 1, \dots, N$.

Positive definite. When $k = N$, we have $K_{N+1} = I$, which is a positive definite matrix. We assume that K_1 is a positive definite matrix. Then we need to prove $K_0 \succ 0$, i.e.,

$$P_0 + W_0^T K_1 W_0 + F_0^T \Gamma_0^T (Q_0 + K_1) \Gamma_0 F_0 + 2W_0^T K_1 \Gamma_0 F_0 \succ 0.$$

For the third and fourth parts of K_0 , we have

$$\begin{aligned}
&F_0^T \Gamma_0^T (Q_0 + K_1) \Gamma_0 F_0 + 2W_0^T K_1 \Gamma_0 F_0 \\
&= W_0^T K_1 \Gamma_0 R_0^{-1} \Gamma_0^T (Q_0 + K_1) \Gamma_0 R_0^{-1} \Gamma_0^T K_1 W_0 \\
&\quad - 2W_0^T K_1 \Gamma_0 R_0^{-1} \Gamma_0^T K_1 W_0 \\
&\stackrel{(s.1)}{=} R_0^{-1} W_0^T K_1 \Gamma_0 [\Gamma_0^T (Q_0 + K_1) \Gamma_0 R_0^{-1} - 2] \Gamma_0^T K_1 W_0 \\
&\stackrel{(s.2)}{=} (R_0^{-1})^2 W_0^T K_1 \Gamma_0 [\Gamma_0^T (Q_0 + K_1) \Gamma_0 - 2R_0] \Gamma_0^T K_1 W_0 \\
&= -R_0^{-1} W_0^T K_1 \Gamma_0 \Gamma_0^T K_1 W_0,
\end{aligned} \tag{27}$$

where (s.1) follows that R_0^{-1} is a positive real number and (s.2) exploits $R_0^{-1} R_0 = 1$. Combined with (27), we next need to prove

$$P_0 + W_0^T K_1 W_0 - R_0^{-1} W_0^T K_1 \Gamma_0 \Gamma_0^T K_1 W_0 \succ 0. \tag{28}$$

Note that the sum of the positive definite matrix is still a positive definite matrix and P_0 is the given positive definite matrix. We only need to show the positive definiteness of the second and third parts of K_0 . Consider that $W_0^T K_1 W_0 - R_0^{-1} W_0^T K_1 \Gamma_0 \Gamma_0^T K_1 W_0$ in (28) can be rewritten as $(W_0^T - R_0^{-1} W_0^T K_1 \Gamma_0 \Gamma_0^T) K_1 (W_0 - R_0^{-1} \Gamma_0 \Gamma_0^T K_1 W_0^T) + (W_0^T - R_0^{-1} W_0^T K_1 \Gamma_0 \Gamma_0^T) K_1 (R_0^{-1} \Gamma_0 \Gamma_0^T K_1 W_0)$.

Let $Z_0 \triangleq W_0 - R_0^{-1} \Gamma_0 \Gamma_0^T K_1 W_0^T$. Then the above result can be transformed as

$$Z_0^T K_1 Z_0 + R_0^{-1} W_0^T K_1 \Gamma_0 (1 - R_0^{-1} \Gamma_0^T K_1 \Gamma_0) \Gamma_0^T K_1 W_0.$$

Since $R_0 = \Gamma_0^T (Q_0 + K_1) \Gamma_0$, we have $1 - R_0^{-1} \Gamma_0^T K_1 \Gamma_0 > 0$. For any non-zero vector $v_0 \in \mathbb{R}^n$, $Z_0 v_0 \neq \mathbf{0}$ holds. Since K_1 is a positive definite matrix, there exists

$$(Z_0 v_0)^T K_1 (Z_0 v_0) > 0.$$

Thus, we have $v_0^T (Z_0^T K_1 Z_0) v_0 > 0$. Since $v_0 \neq \mathbf{0}$, it can be inferred that $Z_0^T K_1 Z_0$ is a positive definite matrix. Similarly, $R_0^{-1} W_0^T K_1 \Gamma_0 (1 - R_0^{-1} \Gamma_0^T K_1 \Gamma_0) \Gamma_0^T K_1 W_0 > 0$ always holds. Hence, (28) is proved and we have $K_k = K_k^* \succ 0$ for $k = 0, 1, \dots, N$. The proof is completed.

C. Proof of Lemma 2

Note that (12) is a sufficient condition to ensure that $\tilde{V}_{k-1} - \tilde{V}_k$ decreases along the convergence direction of matrix $K_k - K^*$ in the discrete-time system. Moreover, given φ_k in (11), if and only if $\tilde{V}_k = 0$, the equality will be zero. Then, (12) can be expressed as

$$\tilde{V}_{k-1} = \tilde{V}_k - \varphi_k \tilde{V}_k^\alpha = \tilde{V}_k (1 - \frac{\varphi_k}{\tilde{V}_k^{1-\alpha}}).$$

Let the initial value of the Lyapunov function be

$$\tilde{V}_N = \beta_N (\varphi_N)^{\frac{1}{1-\alpha}}, \quad \beta_N > 0.$$

Substituting the value \tilde{V}_N in (12), one gets

$$\tilde{V}_{N-1} = \beta_N (\varphi_N)^{\frac{1}{1-\alpha}} - \varphi_N \tilde{V}_N^\alpha = (\beta_N - \beta_N^\alpha) (\varphi_N)^{\frac{1}{1-\alpha}}.$$

Define $\beta_{N-1} = \beta_N - \beta_N^\alpha$. Then we have $\tilde{V}_{N-1} = \beta_{N-1} - \beta_{N-1}^\alpha$. Substituting the above value \tilde{V}_{N-1} into (12), it can be inferred that

$$\tilde{V}_{N-2} = \beta_{N-2} (\varphi_N)^{\frac{1}{1-\alpha}},$$

where $\beta_{N-2} = \beta_{N-1} - a_{N-1} \beta_{N-1}^\alpha$ and $a_{N-1} = \frac{\varphi_{N-1}}{\varphi_N}$.

Similarly, with a recursive relation of β_k for $1 \leq k \leq N$, \tilde{V}_{k-1} can be expressed as

$$\tilde{V}_{k-1} = \beta_{k-1} (\varphi_N)^{\frac{1}{1-\alpha}}, \tag{29}$$

where $\beta_{k-1} = \beta_k - a_k \beta_k^\alpha$ and $a_k = \frac{\varphi_k}{\varphi_N}$. If \tilde{V}_k and φ_k satisfy (11), then we obtain

$$\begin{aligned}
\beta_{k-1} &\leq \beta_k - (1 - \epsilon) \beta_k^\alpha, \\
&= \epsilon \beta_k^\alpha - (1 - \beta_k^{1-\alpha}) \beta_k^\alpha.
\end{aligned}$$

Since $\tilde{V}_{k-1} = \tilde{V}(K_{k-1} - K^*)$ is positive definite, β_{k-1} is non-negative. When $\beta_{k-1} = 0$, it follows that

$$\epsilon = 1 - \beta_k^{1-\alpha} \Leftrightarrow \beta_k^{1-\alpha} = 1 - \epsilon. \tag{30}$$

Let $k = \xi^*$ be the smallest integer for which (30) is satisfied, i.e., $\beta_{\xi^*} = (1 - \epsilon)^{\frac{1}{1-\alpha}}$. In other words, $\beta_{\xi^*-1} = 0$. Thus, it is easy to obtain that $\tilde{V}_k = 0$ with $\beta_k = 0$ for $0 \leq k < \xi^*$. Consequently, K_k converges to K^* inversely in finite-time ξ^* . The proof is completed.

D. Proof of Theorem 2

The proof is completed by utilizing discrete-time Lyapunov analysis. With Corollary 1 and Lemma 2, we just need to find a Lyapunov function \tilde{V}_k , which satisfies the convergence condition in (12). The details are shown below.

We define the non-negative Lyapunov function \tilde{V}_k as

$$\tilde{V}_k = \frac{1}{2} \text{trace}[(K_k - K^*)^T (K_k - K^*)], \quad (31)$$

where K^* is the steady-state matrix of inverse convergence. Let $\tilde{K}_k \triangleq K_k - K^*$. Then we have $\tilde{V}_k = \frac{1}{2} \text{trace}[\tilde{K}_k^T \tilde{K}_k]$. Thus, $\tilde{V}_{k-1} - \tilde{V}_k$ can be rewritten as

$$\begin{aligned} & \tilde{V}_{k-1} - \tilde{V}_k \\ &= \frac{1}{2} \text{trace}[(K_{k-1} - K^*)^T (K_{k-1} - K^*) \\ & \quad - (K_k - K^*)^T (K_k - K^*)], \\ &= \frac{1}{2} \text{trace}[\tilde{K}_{k-1}^T \tilde{K}_{k-1} - \tilde{K}_k^T \tilde{K}_k], \\ &= \frac{1}{2} \text{trace}[(\tilde{K}_{k-1} - \tilde{K}_k)^T (\tilde{K}_{k-1} + \tilde{K}_k)], \\ &= -\frac{\frac{1}{2} \text{trace}[(\tilde{K}_k - \tilde{K}_{k-1})^T (\tilde{K}_{k-1} + \tilde{K}_k)]}{\{\frac{1}{2} \text{trace}[\tilde{K}_k^T \tilde{K}_k]\}^{1/p}} (\tilde{V}_k)^{1/p}. \end{aligned} \quad (32)$$

Let $\frac{1}{2} < 1/p < 1$. To apply Lemma 2, we need to find the upper bound of the term on the right side of equality (32).

Consider the term,

$$\begin{aligned} & \frac{\frac{1}{2} \text{trace}[(\tilde{K}_{k-1} - \tilde{K}_k)^T (\tilde{K}_{k-1} + \tilde{K}_k)]}{\{\frac{1}{2} \text{trace}[\tilde{K}_k^T \tilde{K}_k]\}^{1/p}} \\ & \stackrel{(s.1)}{\leq} \frac{\frac{1}{2} \sqrt{\text{trace}[(\tilde{K}_{k-1} - \tilde{K}_k)^T (\tilde{K}_{k-1} + \tilde{K}_k)]} \sqrt{\text{trace}[(\tilde{K}_{k-1} + \tilde{K}_k)^T (\tilde{K}_{k-1} - \tilde{K}_k)]}}{\{\frac{1}{2} \text{trace}[\tilde{K}_k^T \tilde{K}_k]\}^{1/p}}, \\ & \stackrel{(s.2)}{=} \frac{\{\tilde{V}_k + \tilde{V}_{k-1} - \text{trace}[\tilde{K}_k^T \tilde{K}_{k-1}]\}^{\frac{1}{2}}}{\{\tilde{V}_k + \tilde{V}_{k-1} + \text{trace}[\tilde{K}_k^T \tilde{K}_{k-1}]\}^{\frac{1}{2}}}, \end{aligned} \quad (33)$$

where (s.1) follows the fact that $\text{trace}[A^T B] \leq \{\text{trace}[A^T A]\}^{\frac{1}{2}} \{\text{trace}[B^T B]\}^{\frac{1}{2}}$ for any n -order real symmetric matrix, (s.2) follows the fact that $\text{trace}[\tilde{K}_k^T \tilde{K}_{k-1}] = 2\tilde{V}_k$ and $\text{trace}[A] = \text{trace}[A^T]$. Since $\tilde{V}_{k-1} = \beta_{k-1}(\varphi_N)^{\frac{1}{1-\alpha}}$ in (29) and $\tilde{V}_k = \beta_k(\varphi_N)^{\frac{1}{1-\alpha}}$, one gets

$$\tilde{V}_{k-1} = \eta_k \tilde{V}_k, \quad (34)$$

with $\eta_k = \frac{\beta_{k-1}}{\beta_k} = \frac{\text{trace}[\tilde{K}_{k-1}^T \tilde{K}_{k-1}]}{\text{trace}[\tilde{K}_k^T \tilde{K}_k]}$. In addition, with $\zeta_k = \frac{\text{trace}[\tilde{K}_k^T \tilde{K}_{k-1}]}{\text{trace}[\tilde{K}_k^T \tilde{K}_k]}$, we have

$$\text{trace}[\tilde{K}_k^T \tilde{K}_{k-1}] = \zeta_k \tilde{V}_k. \quad (35)$$

Thus, (33) can be rewritten as

$$\begin{aligned} & \frac{\frac{1}{2} \text{trace}[(\tilde{K}_{k-1} - \tilde{K}_k)^T (\tilde{K}_{k-1} + \tilde{K}_k)]}{\{\frac{1}{2} \text{trace}[\tilde{K}_k^T \tilde{K}_k]\}^{1/p}} \\ & \leq \sqrt{(1 + \eta_k)^2 - (\zeta_k)^2} (\tilde{V}_k)^{1-1/p}. \end{aligned} \quad (36)$$

Since \tilde{K}_k and \tilde{K}_{k-1} are n -order real symmetric matrix from Lemma 1, it follows that

$$\begin{aligned} \text{trace}[\tilde{K}_k^T \tilde{K}_{k-1}] & \leq \left\{ \text{trace}[\tilde{K}_k^T \tilde{K}_k] \right\}^{\frac{1}{2}} \left\{ \text{trace}[\tilde{K}_{k-1}^T \tilde{K}_{k-1}] \right\}^{\frac{1}{2}}, \\ & \leq \sqrt{2\tilde{V}_k} \sqrt{2\tilde{V}_{k-1}}. \end{aligned} \quad (37)$$

Combined (35) with (37), we have

$$\zeta_k \leq 2 \sqrt{\frac{\tilde{V}_{k-1}}{\tilde{V}_k}} = 2\sqrt{\eta_k}.$$

Hence, (36) can be rewritten as

$$\frac{\frac{1}{2} \text{trace}[(\tilde{K}_{k-1} - \tilde{K}_k)^T (\tilde{K}_{k-1} + \tilde{K}_k)]}{\{\frac{1}{2} \text{trace}[\tilde{K}_k^T \tilde{K}_k]\}^{1/p}} \leq |\eta_k - 1| (\tilde{V}_k)^{1-1/p}.$$

One can see that $\tilde{V}_{k-1} - \tilde{V}_k = 0$ if $\eta_k = 1$ or $\tilde{V}_k = 0$. Furthermore, if and only if $\tilde{V}_k = 0$, we conclude that

$$\tilde{V}_{k-1} - \tilde{V}_k = 0 \Leftrightarrow \tilde{K}_k = 0 \Leftrightarrow K_k = K^*.$$

It shows that $\tilde{V}_k = 0$ if and only if K_k is at the equilibrium matrix K^* .

We consider $\tilde{K}_{k-1} = \mu_k \tilde{K}_k$ with $\mu_k > 0$. To guarantee that (12) holds, combined with (32), we have

$$\begin{aligned} \tilde{V}_{k-1} - \tilde{V}_k &= (\mu_k^2 - 1) \tilde{V}_k, \\ &= -[(1 - \mu_k^2) \tilde{V}_k^{1-1/p}] \tilde{V}_k^{1/p}, \end{aligned}$$

where $(1 - \mu_k^2) \tilde{V}_k^{1-1/p}$ is the function of $\tilde{V}_k^{1-\alpha}$ with $\alpha = 1/p$. If μ_k satisfies

$$\mu_k = \frac{(2\tilde{V}_k)^{1-1/p} - \kappa}{(2\tilde{V}_k)^{1-1/p} + \kappa},$$

where $\kappa > 0$, then we have

$$\varphi_k \triangleq (1 - \mu_k^2) \tilde{V}_k^{1-1/p} = 4\kappa \frac{2^{1-1/p} (\tilde{V}_k)^{2-2/p}}{[(2\tilde{V}_k)^{1-1/p} + \kappa]^2}.$$

From (11), \tilde{V}_k is decreasing if $0 < \varphi_k < \frac{4\kappa}{2^{1-1/p}}$ for $\tilde{V}_k^{1-1/p} \in (0, \tilde{V}_N^{1-1/p})$. In addition, the ratio $\frac{\varphi_k}{\varphi_N}$ is bounded and higher than a positive constant in the open interval $(0, 1)$ since

$$\frac{\varphi_k}{\varphi_N} = \left(\frac{\tilde{V}_k}{\tilde{V}_N} \right)^{2-2/p} \frac{[(2\tilde{V}_N)^{1-1/p} + \kappa]^2}{[(2\tilde{V}_k)^{1-1/p} + \kappa]^2}.$$

Therefore, K_k will converge to K^* inversely for $0 \leq k < \xi^*$ where the positive integer ξ^* satisfies (30). Finally, the proof is completed.

REFERENCES

- [1] X.-M. Zhang, Q.-L. Han, X. Ge, D. Ding, L. Ding, D. Yue, and C. Peng, "Networked control systems: A survey of trends and techniques," *IEEE/CAA JAS*, vol. 7, no. 1, pp. 1–17, 2019.
- [2] X. Luo, C. Fang, J. He, C. Zhao, and D. Paccagnan, "A feedback-optimization-based model-free attack scheme in networked control systems," *arXiv preprint arXiv:2212.07633*, 2022.
- [3] G. Darande, "cyberattacks against iran's steel industry," <https://www.youtube.com/watch?v=fnbCr8mgoT8>, 2022.

- [4] Y. Liu, P. Ning, and M. K. Reiter, "False data injection attacks against state estimation in electric power grids," *ACM Trans. Inf. Syst. Secur.*, vol. 14, no. 1, pp. 1–33, 2011.
- [5] Y. Mo and B. Sinopoli, "False data injection attacks in control systems," in *Workshop on Secure Control Syst.*, 2010, pp. 1–6.
- [6] T. Sui, Y. Mo, D. Marelli, X. Sun, and M. Fu, "The vulnerability of cyber-physical system under stealthy attacks," *IEEE TAC*, vol. 66, no. 2, pp. 637–650, 2020.
- [7] Y. Zhu, J. Yan, Y. Tang, Y. L. Sun, and H. He, "Resilience analysis of power grids under the sequential attack," *IEEE TIFS*, vol. 9, no. 12, pp. 2340–2354, 2014.
- [8] R. Tan, H. H. Nguyen, E. Y. Foo, D. K. Yau, Z. Kalbarczyk, R. K. Iyer, and H. B. Gooi, "Modeling and mitigating impact of false data injection attacks on automatic generation control," *IEEE TIFS*, vol. 12, no. 7, pp. 1609–1624, 2017.
- [9] Y. Chen, S. Kar, and J. M. Moura, "Cyber-physical attacks with control objectives," *IEEE TAC*, vol. 63, no. 5, pp. 1418–1425, 2017.
- [10] Y.-G. Li and G.-H. Yang, "Optimal stealthy false data injection attacks in cyber-physical systems," *Inf. Sciences*, vol. 481, pp. 474–490, 2019.
- [11] M. Jafari, M. A. Rahman, and S. Paudyal, "Optimal false data injection attacks against power system frequency stability," *IEEE TSG*, 2022.
- [12] G. Wu, J. Sun, and J. Chen, "Optimal data injection attacks in cyber-physical systems," *IEEE TCYB*, vol. 48, no. 12, pp. 3302–3312, 2018.
- [13] G. Wu, G. Wang, J. Sun, and L. Xiong, "Optimal switching attacks and countermeasures in cyber-physical systems," *IEEE TSMC*, vol. 51, no. 8, pp. 4825–4835, 2019.
- [14] L. Ye, N. Woodford, S. Roy, and S. Sundaram, "On the complexity and approximability of optimal sensor selection and attack for kalman filtering," *IEEE TAC*, vol. 66, no. 5, pp. 2146–2161, 2020.
- [15] X. Luo, C. Zhao, C. Fang, and J. He, "Submodularity-based false data injection attack scheme in multi-agent dynamical systems," in *IEEE ACC*, 2022, pp. 4998–5003.
- [16] X. Luo, C. Fang, C. Zhao, P. Cheng, and J. He, "Optimal sequential false data injection attack scheme: Finite-time inverse convergence," in *IEEE CDC*, 2023.
- [17] Q. Zhang, K. Liu, Y. Xia, and A. Ma, "Optimal stealthy deception attack against cyber-physical systems," *IEEE TCYB*, vol. 50, no. 9, pp. 3963–3972, 2020.
- [18] A.-Y. Lu and G.-H. Yang, "False data injection attacks against state estimation without knowledge of estimators," *IEEE TAC*, vol. 67, no. 9, pp. 4529–4540, 2022.
- [19] X. Luo, C. Fang, C. Zhao, and J. He, "A model-free false data injection attack strategy in networked control systems," in *IEEE CDC*, 2022, pp. 2941–2946.
- [20] J. Kim, L. Tong, and R. J. Thomas, "Subspace methods for data attack on state estimation: A data driven approach," *IEEE TSP*, vol. 63, no. 5, pp. 1102–1114, 2014.
- [21] L. An and G.-H. Yang, "Data-driven coordinated attack policy design based on adaptive \mathcal{L}_2 -gain optimal theory," *IEEE TAC*, vol. 63, no. 6, pp. 1850–1857, 2017.
- [22] Z. Zhao, Y. Xu, Y. Li, Z. Zhen, Y. Yang, and Y. Shi, "Data-driven attack detection and identification for cyber-physical systems under sparse sensor attacks," *IEEE TAC*, 2022.
- [23] E. Mousavinejad, X. Ge, Q.-L. Han, F. Yang, and L. Vlacic, "Resilient tracking control of networked control systems under cyber attacks," *IEEE TCYB*, vol. 51, no. 4, pp. 2107–2119, 2021.
- [24] X.-L. Wang, "Optimal attack strategy against fault detectors for linear cyber-physical systems," *Information Sciences*, vol. 581, pp. 390–402, 2021.
- [25] F. Pasqualetti, F. Dörfler, and F. Bullo, "Attack detection and identification in cyber-physical systems," *IEEE TAC*, vol. 58, no. 11, pp. 2715–2729, 2013.
- [26] Z. Guo, D. Shi, K. H. Johansson, and L. Shi, "Worst-case stealthy innovation-based linear attack on remote state estimation," *Automatica*, vol. 89, pp. 117–124, 2018.
- [27] R. Hamrah, A. K. Sanya, and S. P. Viswanathan, "Discrete finite-time stable position tracking control of unmanned vehicles," in *IEEE CDC*, 2019, pp. 7025–7030.
- [28] M. L. Puterman, "Markov decision processes," *Handbooks in operations research and management science*, vol. 2, pp. 331–434, 1990.
- [29] J. Schulman, F. Wolski, P. Dhariwal, A. Radford, and O. Klimov,

- “Proximal policy optimization algorithms,” *arXiv preprint arXiv:1707.06347*, 2017.
- [30] R. S. Sutton and A. G. Barto, *Reinforcement learning: An introduction*. MIT press, 2018.
- [31] T. P. Lillicrap, J. J. Hunt, A. Pritzel, N. Heess, T. Erez, Y. Tassa, D. Silver, and D. Wierstra, “Continuous control with deep reinforcement learning,” *arXiv preprint arXiv:1509.02971*, 2015.
- [32] J. Schulman, S. Levine, P. Abbeel, M. Jordan, and P. Moritz, “Trust region policy optimization,” in *ICML*, 2015, pp. 1889–1897.
- [33] A. Agarwal, S. M. Kakade, J. D. Lee, and G. Mahajan, “On the theory of policy gradient methods: Optimality, approximation, and distribution shift,” *JMLR*, vol. 22, no. 1, pp. 4431–4506, 2021.
- [34] L. Wang, Q. Cai, Z. Yang, and Z. Wang, “Neural policy gradient methods: Global optimality and rates of convergence,” *arXiv preprint arXiv:1909.01150*, 2019.